A Feasibility Study of Piecewise Phase Variable Based on Variable Toe-Off for the Powered Prosthesis Control: A Case Study

Woolim Hong , *Member, IEEE*, Namita Anil Kumar , Shawanee' Patrick, Sunwoong Moon, and Pilwon Hur

Abstract—Achieving stable walking and proper assistance in prosthesis control requires synchronized control, treating the user and the prosthesis as a coupled system. Furthermore, speed adaptability is essential for controlling the prosthesis at different walking speeds. One approach involves using a phase variable to estimate the user's gait phase and synchronize prosthesis control accordingly. However, the current phase variable (i.e., PV) fails to reflect variable toe-off timing at different speeds, despite individuals having different toe-off timings per walking speed. To address this issue, we propose a piecewise phase variable (i.e., PW-PV) that accounts for different toe-off timings while estimating the user's gait phase at various speeds. We conducted a treadmill walking experiment with two participants (one healthy and one amputee) using a custom-built powered prosthesis to validate the PW-PV's feasibility. We collected and analyzed joint kinematics, kinetics, and ground reaction force data during the experiment. The PW-PV implementation resulted in faster load transfer and a more natural rollover for both participants during walking. This allowed healthy and amputee participants to experience longer push-off durations of 10.6% and 15.2%, respectively, and greater ankle push-off work of 7.3% and 16.9%. Furthermore, with the PW-PV, the amputee participant demonstrated higher vertical ground reaction forces of 5.4% and 4.7% on her prosthesis side leg during load acceptance and push-off periods, potentially suggesting increased confidence in using the prosthesis. We anticipate that by using the proposed phase variable, we will be able to provide more appropriate and timely assistance to individuals at variable walking speeds.

Index Terms—Wearable robotics, rehabilitation robotics, prosthetics and exoskeletons, phase variable.

I. INTRODUCTION

EVEN if they are not aware of it, healthy humans walk stably and comfortably. On the other hand, lower-limb amputee patients have limited mobility and dexterity in their daily lives, leaving them vulnerable to falls and injuries [1], [2], [3]. It may also prevent amputees from participating in social activities due to reduced mobility [1], [4]. As a result, lower-limb amputation would have a significant psychological and physical impact on patients. There were over 600,000 people in the United States living with a major lower-limb amputation in 2005, and this number is predicted to double by 2050 [5]. Worldwide, this growth is expected to reach more than a million due to the global prevalence of diabetes by 2030 [6]. Lower-limb prostheses have evolved and are widely used to replace missing limbs in order to restore amputees' mobility, stability, and community participation [1], [4]. Powered prostheses (i.e., robotic prostheses) have been developed and studied by researchers for decades as a treatment to restore their gaits as closely as possible to those of healthy people in broader walking scenarios: level walking [7], [8], [9], [10], slope walking [11], [12], [13], and stair walking [14], [15]. When controlling powered prostheses, real-time estimation of the user's gait phase is paramount for synchronized control with the user. Failure to achieve such synchronization can lead to instability and inadequate assistance to the user while ambulating [16], [17].

A learning-based estimation is one approach for estimating the user's gait phase. Recent advances in machine learning allow researchers to improve the accuracy and robustness of estimating the user's gait phase [18], [19]. Because they use a high-dimensional kinematics and kinetics dataset for model training, this approach can present the user's gait behavior more precisely and robustly. This yields a continuous gait phase estimation, which is preferable to a discrete gait phase estimation for the seamless control of lower-limb wearable devices [20], [21], [22]. However, due to its high computational cost, processing time should be carefully managed for real-time usage [19].

Phase variable is another approach that has been widely utilized in controlling powered prostheses [9], [23], [24], [25]. Different kinematic information can be used to compute the phase variable, such as hip position [7] or thigh information [13], [23]. The phase variable computation is straightforward, allowing for instant estimation and real-time control of the prosthesis. This variable can also adapt to different walking speeds based

on the user's kinematics during the gait cycle [9], [13], [23]. The duration of heel-strike (i.e., stride time) can also be used to estimate the walking speed. Even though this existing phase variable can adapt to different walking speeds based on the user's kinematics and different stride times, variable toe-off timing per different speeds has never been considered.

Several attempts have been made to incorporate toe-off timing into the generation of a piecewise phase variable [26], [27], [28]. The concept of the piecewise phase variable was first introduced by Villarreal et al. to enable voluntary control over non-rhythmic movements such as starting/stopping and stepping forward/backward [26]. By dividing the gait cycle into two phases (i.e., stance and swing) and defining the piecewise phase variable using the thigh angle based on pre-defined toe-off timing (i.e., 0.57), they were able to control non-rhythmic motions. However, their focus was on non-rhythmic motions, not walking itself.

Other researchers have demonstrated that the piecewise phase variable can be used for different walking speeds [27] and different locomotion modes [28]. They divided the gait cycle into three phases (i.e., stance, swing, and retraction) based on the characteristics of the thigh angle [27], [28]. To define the piecewise phase variable, they used an optimized sigmoid function for the stance and swing phases and a constantly increasing function for the retraction phase. They then applied the Kalman filter to smooth their resulting phase variable. They demonstrated that their piecewise phase variable could be used at various walking speeds [27] and for slope and stair walking [28]. However, in controlling the prosthesis, they both utilized pre-defined ankle and knee trajectories to follow, which may not be appropriate for each user as individuals have different trajectories, especially amputees [29]. Therefore, it is necessary to be more adaptive to the user's gait in real time rather than relying on pre-defined human trajectories.

User adaptability should be addressed more in variable speed conditions because the user's gait is also changed per speed; it is widely known, for example, that individuals exhibit varying toe-off timings at different walking speeds [30], [31]. A recent study has demonstrated that incorporating toe-off timing into the user's gait phase estimation could enhance its estimation accuracy and speed adaptability [32]. Motivated by this finding, we propose a novel piecewise phase variable (i.e., PW-PV) that can be adjusted for variable toe-off according to walking speed. The contributions of this study are to check the feasibility of i) variable toe-off detection at each gait cycle and ii) slope adjustment of phase variable based on toe-off, and to examine iii) the effect of the proposed method on joint kinematics, kinetics, and ground reaction force results. To achieve these objectives, in Section II, we describe the conventional phase variable (i.e., PV) and the proposed PW-PV computation procedure based on the user's thigh kinematics and toe-off information. This section also provides an overview of our powered prosthetic system, including the hardware and control framework. In Sections III and IV, we present the experimental protocols and results, respectively. We discuss the implications of our findings and the limitations of our study in Section V and conclude the study in Section VI.

II. METHOD

Thigh information is one of the most popular choices for phase variable computation [9], [23], [24], [25]. The basic idea behind using thigh information to compute phase variables is that the phase portrait of the thigh angular position and its integral profiles is shaped like an ellipse. This section describes two different phase variables: the conventional phase variable (i.e., PV) and the piecewise phase variable (i.e., PW-PV). Both methods require the inertial and force sensors to estimate the user's gait phase, which will be explained in more detail in the subsection on hardware and control frameworks for powered prosthetic systems.

A. Phase Variable (PV)

When using the thigh to compute the phase variable, two basic assumptions are given: i) a thigh profile during the gait cycle (i.e., $\theta(t)$) is similar to the cosine function, ii) its integral profile (i.e., $\Theta(t) = \int \theta(t)\, dt$) is similar to the sine function. Thus, the phase portrait of these two profiles is shaped like an ellipse. A phase variable is calculated using the arc-tangent function, as shown below:

$$\phi(t) = \frac{1}{2\pi} atan2(k(\Theta(t) - \alpha), (\theta(t) - \beta)), \quad (1)$$

where the normalizing factors (k, α, and β) are defined by

$$k = \frac{|\theta_{\max} - \theta_{\min}|}{|\Theta_{\max} - \Theta_{\min}|},$$

$$\alpha = \frac{|\Theta_{\max} + \Theta_{\min}|}{2}, \; \beta = \frac{|\theta_{\max} + \theta_{\min}|}{2}. \quad (2)$$

Note that k, α, and β represent the scale coefficient, the amplitude shift of the thigh integral, and that of the thigh angle, respectively. These normalizing factors help the center of the phase portrait ($\theta(t)$ vs. $\Theta(t)$) be around the origin and reduce the non-linearity of the phase variable by maintaining the orbital radius of the phase portrait. The integral value is initialized when heel-strike occurs, and the normalizing factors are updated at each gait cycle. We refer to the conventional phase variable produced by this procedure as PV and denote it as $\phi(t)$ throughout this paper. To make $\phi(t)$ bounded on [0,1], the final $\phi(t)$ is generated as below:

$$\phi(t) = \begin{cases} \phi(t) & \text{for } \phi(t) \geq 0 \\ \phi(t) + 1 & \text{for } \phi(t) < 0 \end{cases} \quad (3)$$

B. Piecewise Phase Variable (PW-PV)

One of the key benefits of using PV is that it can represent the user's walking state as a percentage, regardless of their walking speed, by analyzing their kinematics [23], [25]. This allows PV to estimate the user's walking state when their kinematics change per walking speed. However, as the PV is computed solely on kinematics information, it has limitations in detecting some important events such as heel-off and toe-off, which are known to vary depending on walking speed [30], [31]. To address this issue, we propose a new approach called piecewise phase variable, denoted PW-PV, in this study. Unlike the conventional PV,
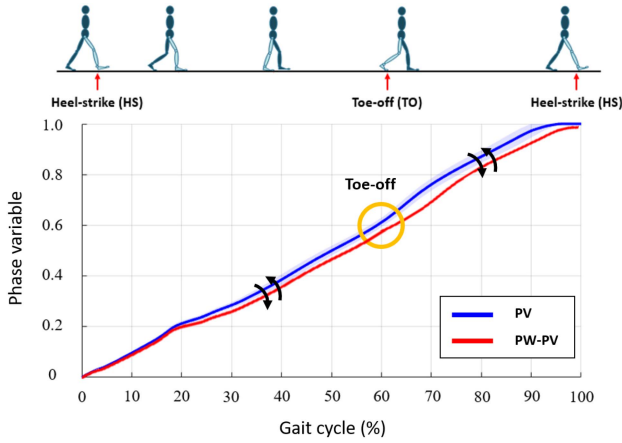
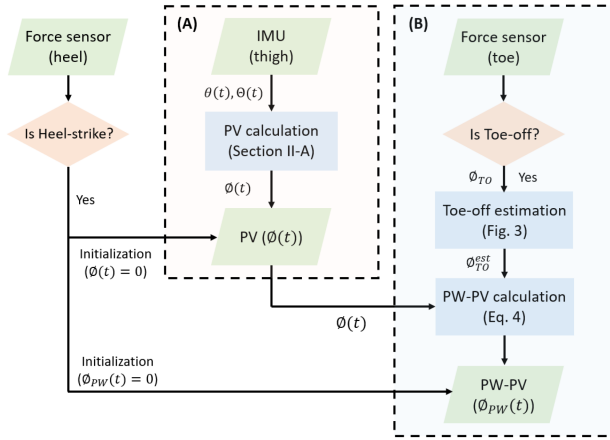Fig. 1. Slope adjustment based on toe-off in PW-PV. Blue indicates the PV, while red indicates the PW-PV.

Fig. 2. Flowchart of PV and PW-PV computation: (a) PV computation process. (b) PW-PV computation using $\phi(t)$ and ϕ_{TO}^{est}. Heel-strike initiates the PV and PW-PV to start the new gait cycle.
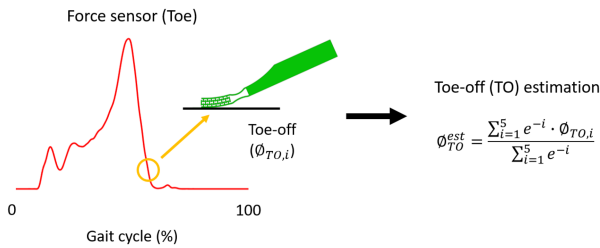

Fig. 3. Toe-off estimation using a force sensor at the toe. Five prior toe-off values were saved and used to calculate the estimated toe-off (ϕ_{TO}^{est}).

the PW-PV tracks toe-off onset timings and uses the estimated toe-off timing to implement slope adjustment when computing the phase variable (see Fig. 1).

Fig. 2 describes the PV and PW-PV computation processes; we performed the same process to get $\phi(t)$, then adjusted the slope of PV based on the estimated toe-off timing (i.e., ϕ_{TO}^{est}) to obtain the PW-PV ($\phi_{PW}(t)$). Fig. 3 depicts the toe-off timing estimation procedure. Using a force sensor at the toe, we
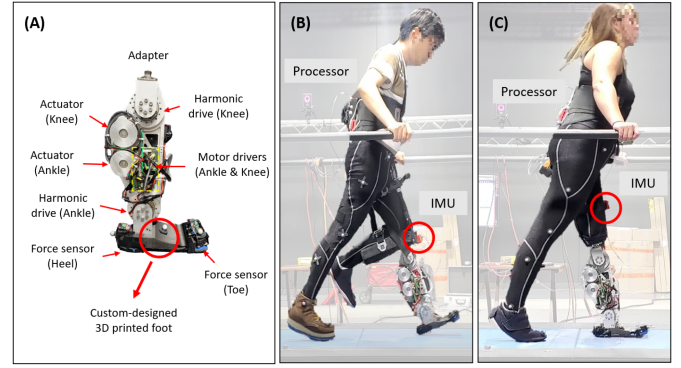

Fig. 4. (a) AMPRO II: a custom-built powered transfemoral prosthesis at Texas A&M University. (b) A healthy participant using an L-shape adapter. (c) An amputee participant using her own socket.

continued to detect toe-off and saved the detected toe-off timings (i.e., $\phi_{TO,i}$) from five previous gaits ($i = 1, 2, \ldots, 5$). A weighted average of these five prior toe-off values was used to estimate toe-off. The weighting is determined by a forgetting factor of e^{-i}, where i represents the ith prior toe-off value. The initial condition of toe-off timing was set as 0.6, referring to 60% of the gait cycle based on human data [30], [31]. Starting from 0.6, toe-off timing is updated every gait cycle to be used for estimating the user's toe-off timing (ϕ_{TO}^{est}), as explained in (4).

$$\phi_{PW}(t) = \begin{cases} \frac{0.6}{\phi_{TO}^{est}} \phi(t) & \phi(t) < \phi_{TO}^{est} \\ \frac{0.4 \cdot (\phi(t) - \phi_{TO}^{est})}{1 - \phi_{TO}^{est}} + 0.6 & \phi(t) \geq \phi_{TO}^{est} \end{cases} \quad (4)$$

C. Powered Prosthetic System

1) Hardware: A custom-built powered transfemoral prosthesis, AMPRO II (Fig. 4(a)), was operated by a micro-processor (BeagleBone Black, Texas Instruments, Dallas, TX, USA) to control the actuated ankle and knee joints. An inertial measurement unit (IMU; MPU 9150, SparkFun Electronics, Niwot, CO, USA) mounted on the user's thigh measures the thigh segment angle (Fig. 4(b) and 4(c))), which is used for PV and PW-PV calculations. A total of three force sensors (FlexiForce A502, Tekscan, South Boston, MA, USA; one at the heel and two at the toe) placed under the prosthetic foot detect the user's heel-strike (HS), flat-foot (FF), heel-off (HO), and toe-off (TO) timings. To increase the sensitivity of toe detection, we placed two force sensors at the toe and took their average to get a final toe force value. These flat, square-shaped sensors have a large sensing area, allowing us to easily capture the moment the participants put their weights on/off the prosthesis. Force sensor thresholds were heuristically determined to identify the gait phases reliably. The HS was utilized as the cue to start the gait cycle; thus, all the sensor data, including IMU and force sensors, was parameterized in the percentage of the gait cycle based on each HS, attaining synchronization of sensor data. The actual ankle/knee joint kinematics and kinetics of the prosthesis side were collected by two high-resolution optical encoders (E5, US Digital, Vancouver, WA, USA) and two motor drivers

TABLE I
THE STIFFNESS AND DAMPING POLYNOMIAL COEFFICIENTS

	$i = 4$	$i = 3$	$i = 2$	$i = 1$	$i = 0$
Ankle k_i	-1.51E+4	1.40E+4	-3.21E+3	3.29E+2	80.0
Ankle d_i	6.36E+2	-8.18E+2	3.45E+2	-5.25E+1	2.71
Knee k_i	9.77E+3	-4.09E+3	-4.63E+3	2.16E+3	20.0
Knee d_i	8.69E+1	-1.39E+2	6.48E+1	-2.82E+0	0.13

TABLE II
EQUILIBRIUM ANGLES FOR EACH GAIT PHASE

	Amputee participant			Healthy participant		
	HS-FF	FF-HO	HO-TO	HS-FF	FF-HO	HO-TO
Ankle	0°	-2°	-10°	2°	-5°	-12°
Knee	10°	8°	14°	10°	6°	14°

(Gold-Solo Whistle, Elmo Motion Control, Petach-Tikva, Israel). The 3D printed foot with a toe joint was equipped to mimic human walking biomechanics [33], [34].

2) Control Framework: AMPRO II was controlled based on the user's gait phase under two control frameworks: impedance control and proportional-derivative (PD) control [25], [35]. All of the impedance parameters (i.e., stiffness and damping coefficients) and desired trajectories were parameterized between the HS using the phase variable $\left(\hat{\phi} \in [0, 1] \right)$, so they were provided in a synchronized manner based on the user's gait phase. Also, these control parameters were initialized based on HS to start the new gait cycle. Note that $\hat{\phi} = \phi$ for PV, while $\hat{\phi} = \phi_{PW}$ for PW-PV.

An impedance controller was utilized while the prosthesis was in contact with the ground (i.e., stance phase) to generate a human-like joint torque for each joint based on the user's walking state [35] as follows:

$$\tau = K(\hat{\phi}) \cdot (\theta_{act} - \theta_{eq}) + D(\hat{\phi}) \cdot \dot{\theta}_{act}, \quad (5)$$

where $K(\hat{\phi})$ and $D(\hat{\phi})$ refer to the joint stiffness and damping parameters. θ_{eq} refers to the equilibrium angle. θ_{act} and $\dot{\theta}_{act}$ are the joint position and velocity measured by the optical encoders. We provided fourth-order stiffness $K(\hat{\phi})$ and damping $D(\hat{\phi})$ polynomials for each joint to have seamless torques for both ankle and knee, as shown in (6). These polynomials are the function of $\hat{\phi}$, so they are continuously varying according to the user's gait progression.

$$K(\hat{\phi}) = \sum_{i=0}^{4} k_i \hat{\phi}^i, \quad D(\hat{\phi}) = \sum_{i=0}^{4} d_i \hat{\phi}^i \quad (6)$$

The stiffness and damping polynomial coefficients were given by k_i and d_i, respectively, and these parameters were estimated by a least squares method based on the human ankle and knee torque profile [35] (see Table I).

To provide the user with proper control, appropriate equilibrium angles (θ_{eq}) also should be assigned for each gait phase. We have three phases during the stance phase based on gait events: HS to FF, FF to HO, and HO to TO. Table II shows the equilibrium angles that have been assigned.

A PD controller was utilized while the prosthesis had no contact with the ground (i.e., swing phase) to follow the desired human-like joint trajectories [13] as follows:

$$\tau = K_p \cdot (\theta_{act} - \theta_{des}(\hat{\phi})) + K_d \cdot (\dot{\theta}_{act} - \dot{\theta}_{des}(\hat{\phi})), \quad (7)$$

where K_p and K_d refer to the proportional and derivative gains, respectively. This ensures sufficient foot clearance during the swing phase. We utilized the same K_p gain values for the ankle and knee ($K_p = 250$) and different K_d gains for the ankle ($K_d = 10$) and knee ($K_d = 20$); these gain values were obtained empirically. $\theta_{des}(\hat{\phi})$ and $\dot{\theta}_{des}(\hat{\phi})$ denote the desired human-like position and velocity trajectories of each joint, while θ_{act} and $\dot{\theta}_{act}$ denote the actual joint position and velocity. Cubic Bezier polynomials were used to generate the desired trajectories for each joint as follows:

$$\theta_{des}(\hat{\phi}) = \sum_{i=0}^{n} \binom{n}{i} (1 - \hat{\phi})^{n-i} \hat{\phi}^i P_i, \quad (8)$$

where $\binom{n}{i}$ are the binomial coefficients ($n = 3$). P_0 refers to the joint positions at TO, measured by the optical encoders, and $P_1 - P_3$ were determined based on the offline optimization, described in [13], for foot clearance during swing phase.

III. EXPERIMENTAL PROTOCOLS

A. Experiment Design

An indoor walking experiment was conducted with a healthy participant (male, 32 yrs, 170 cm, 70 kg) and a participant with traumatic transfemoral amputation (female, 23 yrs, 164 cm, 66 kg w/o prosthesis), as depicted in Fig. 4(b) and 4(c). The amputee participant has been using an Ottobock X3 Knee in conjunction with a Freedom Runway. All walking trials were carried out on an instrumented treadmill (Tandem, AMTI, Watertown, MA, USA), while a 44 camera-based Vicon system (Vantage V5, Vicon, Hauppauge, NY, USA) collected the participants' motion data. Before the experimental data collection, the participants underwent eight training sessions to get used to the powered prosthesis and its control framework. Each training session consisted of 5-6 trials and lasted an hour. For each trial, the participants walked for 1-2 minutes, and 10-15 minutes of break time was provided between trials. Note that the healthy participant had relatively more experience walking with the given prosthesis but not with the proposed method, so he underwent the same procedure as the amputee participant. During the data collection, the participants were asked to walk for 90 seconds for each trial, and 15 minutes of break time was given between trials. To avoid fatigue and potential safety issues, the participants walked at their preferred speed (i.e., 0.67 m/s) throughout all trials. In addition, the participants' safety was ensured with handrails on either side of the treadmill. The participants' motion data was collected and gap-filled in Vicon Nexus, and then the associated anthropomorphic model was reconstructed using Visual 3D (C-Motion, Germantown, MD, USA). The marker and ground reaction force data were filtered using a third-order Butterworth low-pass filter with 10 and 20 Hz cutoff frequencies, respectively. All the joint kinematics and kinetics computations were performed in the sagittal plane. All the experiment protocols have been reviewed and approved by
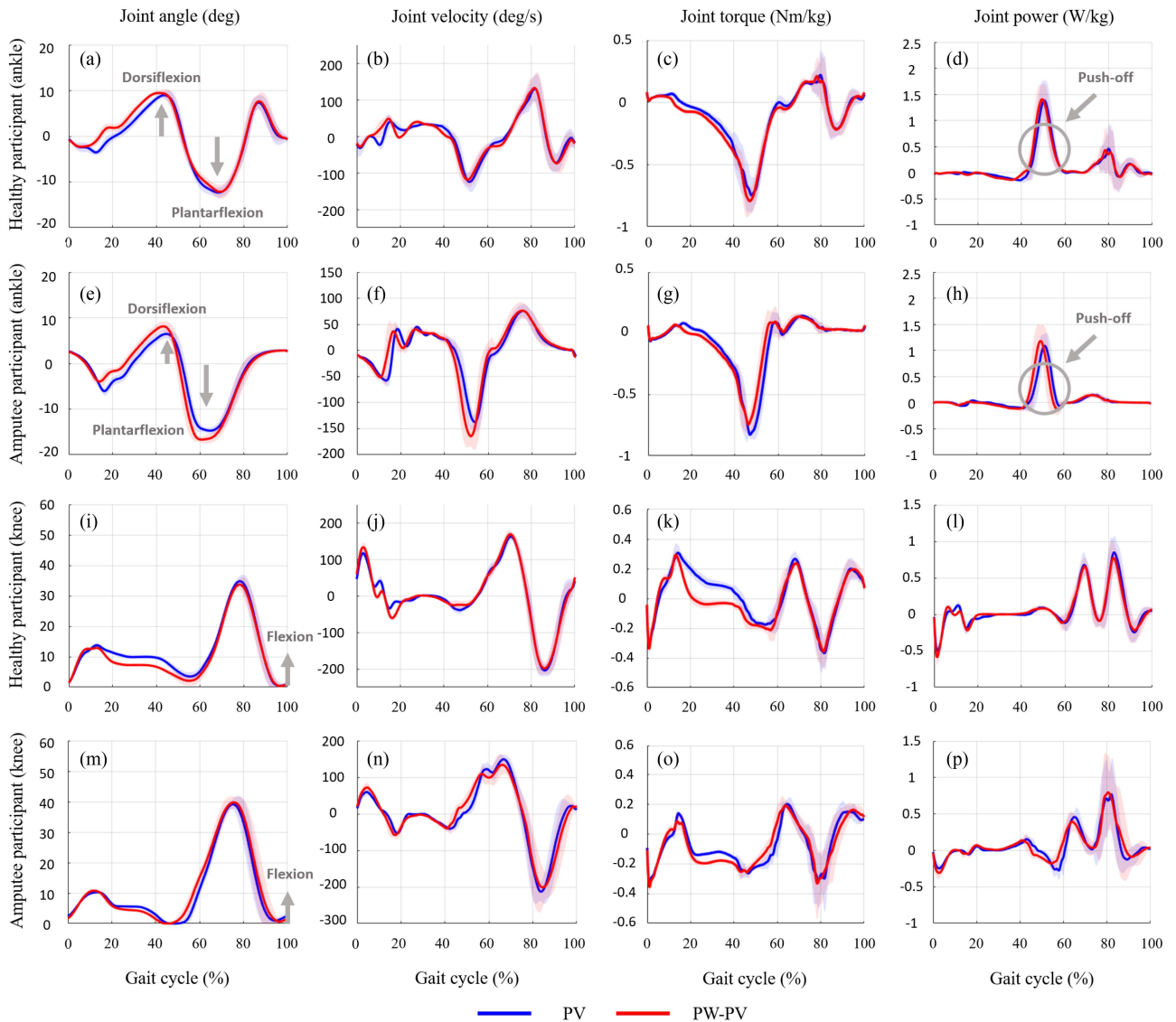
Fig. 5. Prosthesis side joint kinematics/kinetics: (a)–(d) Healthy participant ankle, (e)–(h) Amputee participant ankle, (i)–(l) Healthy participant knee, (m)–(p) Amputee participant knee. Results presented as mean ± SD (shaded region) of 20 consecutive gaits. Blue indicates the PV, while red indicates the PW-PV.

the Institutional Review Board (IRB) at Texas A&M University (IRB2015-0607F).

IV. RESULTS

A. Prosthesis Side Kinematics/Kinetics

As shown in Fig. 5(a) and 5(e), both participants showed earlier ankle dorsiflexion when the PW-PV was utilized. Also, greater dorsiflexion and plantarflexion can be found with the PW-PV, even with a smaller maximum ankle torque in the amputee participant case (Fig. 5(e)–5(g)). The healthy participant also showed greater dorsiflexion with the PW-PV, while his plantarflexion and ankle maximum torque were similar regardless of the methods (Fig. 5(a)–5(c)). Relatively earlier knee flexion is also found with the PW-PV in Fig. 5(i)–(k). According to Fig. 5(k) and 5(o), the prosthesis knee torque showed an apparent

difference between the two methods for both participants. To be more specific, in Fig. 5(k), the PW-PV demonstrated knee extension torque, whereas the PV demonstrated knee flexion torque during 20–40% of the gait cycle. The amputee had knee extension torque regardless of method, as shown in Fig. 5(o), but the PW-PV exhibited more extension torque during this region.

According to Fig. 5(d), the average ankle peak power of the PV and PW-PV did not show a noticeable difference (PV: 1.680±0.253 W/kg vs. PW-PV: 1.651±0.187 W/kg). Additionally, the timings of ankle peak power were similar between the two methods (PV: 49.35±1.65 % vs. PW-PV: 48.70±1.53 %). However, for the amputee participant, the PW-PV resulted in 13.89% greater ankle peak power compared to the PV (Fig. 5(h); PV: 1.375±0.161 W/kg vs. PW-PV: 1.565±0.157 W/kg). Furthermore, the ankle peak power timing was earlier in the PW-PV (PV: 50.72±1.50 % vs. PW-PV: 49.12±1.84 %).
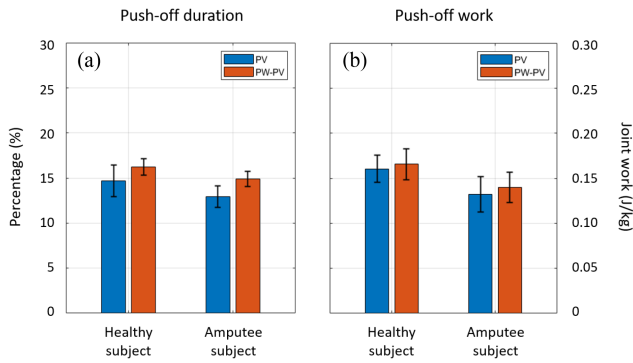
Fig. 6. Prosthesis side push-off duration and work: (a) Push-off duration in the percentage, (b) Normalized ankle push-off work. Blue bar indicates PV result, while red bar indicates PW-PV result.
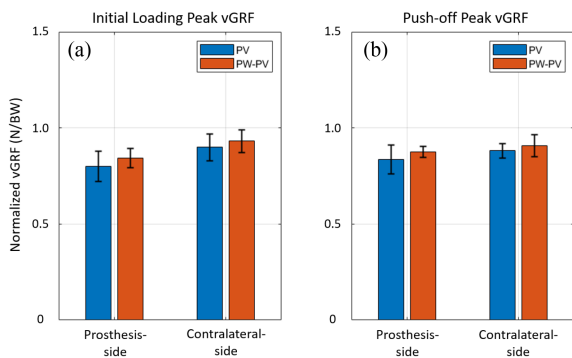

Fig. 7. Normalized vGRFs of the amputee participant: (a) Initial peak loading vGRF, (b) Push-off peak vGRF. The prosthesis side refers to the prosthetic limb, while the contralateral side refers to her intact limb. Blue indicates PV result, while red indicates PW-PV result.

The push-off phase in Fig. 5(d) and 5(h) is essential as it contributes positively to the user's forward propulsion, accounting for about 20% of the gait cycle [36], [37]. As shown in Fig. 6(a), the PW-PV had 10.58% and 15.18% longer push-off duration (i.e., closer to 20%) than the PV for the healthy and amputee participants, respectively. Owing to the longer and timely push-off, the PW-PV provided 7.33% and 16.95% more ankle push-off work to the participants in Fig. 6(b). Fig. 7 depicts the vertical ground reaction force (vGRF) results of the amputee participant. The initial peak loading vGRF refers to the peak vGRF captured when the participant places her weight on one of her legs following heel-strike. The push-off peak vGRF refers to the maximum vGRF during the push-off region. According to Fig. 7, greater vGRFs tend to be found on the prosthesis side in both the initial and push-off peak vGRF results, while the other side (i.e., contralateral side) tends not to be much different.

B. Contralateral Side Kinematics

Fig. 8 shows the kinematics of both participants' contralateral (i.e., intact side) limbs. Both participants made earlier and larger ankle dorsiflexions before push-off with the PW-PV in Fig. 8(a) and 8(c). The healthy participant showed a more dynamic movement at his ankle and greater knee flexion during the stance
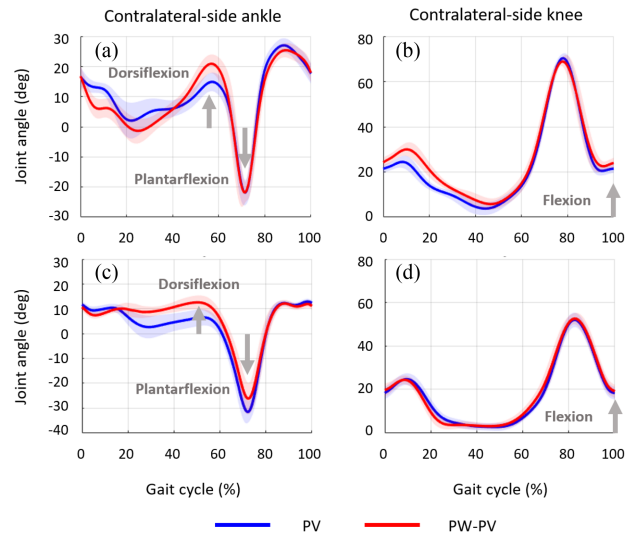

Fig. 8. Contralateral side ankle and knee kinematics: (Top) Healthy participant, (Bottom) Amputee participant. Solid line and shaded region represent mean and ± SD of 20 gaits, respectively. Blue line indicates the PV, while red line indicates the PW-PV.

phase with the PW-PV, as shown in Fig. 8(a) and 8(b). The amputee participant, on the other hand, showed little difference in knee kinematics while having less ankle plantarflexion during push-off with the PW-PV, as illustrated in Fig. 8(c) and 8(d).

V. DISCUSSION

In Fig. 5, it is observed that both participants exhibited earlier ankle dorsiflexions and relatively earlier knee flexions when using the PW-PV, indicating faster load transfer because of slope adjustment. Furthermore, as illustrated in Fig. 5(o), the amputee participant had a higher extension torque with the PW-PV. This extension torque supported the body weight during mid-stance, enabling the participant to move forward with the extended knee. This torque trend is consistent with human data [38], [39].

We found the greater push-off work results with the PW-PV for both participants in Fig. 6 owing to the longer and more timely push-off. This is further supported by the higher peak vGRF observed when the amputee participant made the push-off with the PW-PV, as shown in Fig. 7(b). This could be linked to the earlier and larger ankle dorsiflexions on the contralateral side of both participants in Fig. 8(a) and 8(c). Both participants could benefit from the greater push-off from the prosthesis and made faster load transfer on the contralateral side, leading to the earlier and larger ankle dorsiflexion. Additionally, Fig. 7(a) indicates a greater initial peak vGRF, which refers to weight acceptance when the body weight is fully applied to the stance leg, potentially implying that the amputee participant may trust the prosthesis more and be willing to put more weight on it when walking with the PW-PV.

As shown in Table III, both the PV and PW-PV exhibited high linearity with a small root-mean-square error (RMSE). Although the PW-PV exhibited slightly higher linearity than the PV, the difference was not substantial. However, both

TABLE III
COMPARISON OF TWO METHODS: PV AND PW-PV

PV method	Healthy participant		Amputee participant	
	PV	PW-PV	PV	PW-PV
Linearity (R^2)	0.9921 ± 0.0051	0.9935 ± 0.0040	0.9945 ± 0.0035	0.9962 ± 0.0025
Linearity (RMSE)	$2.14E\text{-}3 \pm 5.20E\text{-}4$	$1.97E\text{-}3 \pm 5.87E\text{-}4$	$2.15E\text{-}3 \pm 6.63E\text{-}4$	$2.15E\text{-}3 \pm 5.99E\text{-}4$
Prosthesis stride time (s)	1.5493 ± 0.0371	1.4900 ± 0.0366	1.6900 ± 0.0303	1.6213 ± 0.0416
Intact stride time (s)	1.5905 ± 0.0408	1.5348 ± 0.0792	1.7221 ± 0.0472	1.6522 ± 0.0608
Heel-strike deviation (s)	0.0900 ± 0.0265	0.0741 ± 0.0309	0.1296 ± 0.0456	0.0879 ± 0.0351

participants had noticeable differences in stride time between the two methods. Stride time refers to the duration of the gait cycle on the prosthesis side and is one of the clinically relevant outcome measures used to evaluate the walking performance of prosthesis users [29], [40]. When the PW-PV was used, the average stride time was reduced by 3.98% and 4.24% for healthy and amputee participants on their prosthesis side, respectively. Moreover, their stride time on the intact side was also decreased with the PW-PV. These results could be attributed to the faster load transfer that occurred with the PW-PV. These findings may also be linked to heel-strike deviation, which is the temporal difference between the actual heel-strike (sensed by the force plate) and the estimated heel-strike (when the PV or PW-PV is maxed out). The PW-PV has smaller deviations from the actual heel-strike for both healthy (14.46%) and amputee (47.44%) participants.

In this study, we recruited two participants to test the feasibility of the proposed method. However, it is worth noting that these two participants are in totally different conditions because one is a healthy participant, and the other is an amputee participant. Also, they had different levels of experience with our device. As aforementioned, the amputee participant went through eight practice sessions to become accustomed to the powered prosthesis and its control framework. Because the healthy participant had been exposed to our prosthetic system for a longer period of time than the amputee participant, the former was more accustomed to walking with the given device. For instance, he could walk without looking down at the ground, even at a faster speed, by using some auditory feedback (i.e., motor sound) from the system. The amputee participant, on the other hand, felt more at ease looking down at the ground to check her heel-strike while walking. She also kept her hands on the handrails while walking. Even after two months of training to get used to the device, she felt more secure holding the handrails because it was her first experience with a powered prosthesis. Some of our results (e.g., vGRFs) may be affected as a result; however, both participants were in the same condition (i.e., holding handrails), alleviating concerns about comparing the two methods. In the future, a harness should be considered to ensure better safety while participants walk without holding the handrails.

As a case study, this study consists of two participants, including only a single amputee. A larger number of amputee participants is needed to draw some statistical conclusions about the proposed method. Therefore, we plan to recruit more participants for the follow-up study. Furthermore, we anticipate having more speed conditions to investigate the performance difference between the two methods at different walking speeds.

VI. CONCLUSION

The primary aim of this study was to develop a prosthesis control system that is adaptive to changes in walking speed by incorporating variable toe-off timings in the phase variable used for control. The conventional phase variable (i.e., PV) is based on stride time and thigh movement, but it does not account for changes in toe-off timings at different walking speeds. To address this limitation, we developed a piecewise phase variable (i.e., PW-PV) that can adjust to different toe-off timings for different walking speeds. We validated the feasibility of the PW-PV through a prosthetic walking experiment involving a healthy participant and an amputee participant. We measured and analyzed the effects of the PW-PV on joint kinematics, kinetics, and ground reaction forces. As a result, the PW-PV enabled faster load transfer with more natural rollover during walking for both participants, leading to longer push-off duration and increased push-off work while walking. Furthermore, the amputee participant exhibited higher ground reaction forces on her prosthesis-side leg, potentially implying increased trust in the prosthesis when the PW-PV was used. We conclude that the proposed phase variable has the potential to provide more appropriate and timely assistance with the prosthesis for individuals with variable walking speeds.

ACKNOWLEDGMENT

REFERENCES

[1] W. C. Miller, A. B. Deathe, M. Speechley, and J. Koval, "The influence of falling, fear of falling, and balance confidence on prosthetic mobility and social activity among individuals with a lower extremity amputation," *Arch. Phys. Med. Rehabil.*, vol. 82, no. 9, pp. 1238–1244, 2001.

[2] C. Gauthier-Gagnon, M.-C. Grisé, and D. Potvin, "Enabling factors related to prosthetic use by people with transtibial and transfemoral amputation," *Arch. Phys. Med. Rehabil.*, vol. 80, no. 6, pp. 706–713, 1999.

[3] L. A. Talbot, R. J. Musiol, E. K. Witham, and E. J. Metter, "Falls in young, middle-aged and older community dwelling adults: Perceived cause, environmental factors and injury," *BMC Public Health*, vol. 5, no. 1, pp. 1–9, 2005.

[4] T. Pohjolainen, H. Alaranta, and M. Kärkäinen, "Prosthetic use and functional and social outcome following major lower limb amputation," *Prosthetics Orthotics Int.*, vol. 14, no. 2, pp. 75–79, 1990.

[5] K. Ziegler-Graham, E. J. MacKenzie, P. L. Ephraim, T. G. Travison, and R. Brookmeyer, "Estimating the prevalence of limb loss in the United States: 2005 to 2050," *Arch. Phys. Med. Rehabil.*, vol. 89, no. 3, pp. 422–429, 2008.

[6] "Amputee statistics you ought to know," Accessed: Dec. 2, 2021. [Online]. Available: https://advancedamputees.com/amputee-statistics-you-ought-know

[7] H. Zhao, J. Reher, J. Horn, V. Paredes, and A. D. Ames, "Realization of nonlinear real-time optimization based controllers onself-contained transfemoral prosthesis," in *Proc. ACM/IEEE 6th Int. Conf. Cyber- Phys. Syst.*, 2015, pp. 130–138.

[8] F. Sup, A. Bohara, and M. Goldfarb, "Design and control of a powered transfemoral prosthesis," *Int. J. Robot. Res.*, vol. 27, no. 2, pp. 263–273, 2008.

[9] R. D. Gregg, T. Lenzi, L. J. Hargrove, and J. W. Sensinger, "Virtual constraint control of a powered prosthetic leg: From simulation to experiments with transfemoral amputees," *IEEE Trans. Robot.*, vol. 30, no. 6, pp. 1455–1471, Dec. 2014.

[10] N. Anil Kumar, S. Patrick, W. Hong, and P. Hur, "Control framework for sloped walking with a powered transfemoral prosthesis," *Front. Neurorobot.*, vol. 15, 2022, Art. no. 790060.

[11] F. Sup, H. A. Varol, and M. Goldfarb, "Upslope walking with a powered knee and ankle prosthesis: Initial results with an amputee subject," *IEEE Trans. Neural Syst. Rehabil. Eng.*, vol. 19, no. 1, pp. 71–78, Feb. 2011.

[12] V. Paredes, W. Hong, S. Patrick, and P. Hur, "Upslope walking with transfemoral prosthesis using optimization based spline generation," in *Proc. IEEE/RSJ Int. Conf. Intell. Robots Syst.*, 2016, pp. 3204–3211.

[13] W. Hong, V. Paredes, K. Chao, S. Patrick, and P. Hur, "Consolidated control framework to control a powered transfemoral prosthesis over inclined terrain conditions," in *Proc. IEEE Int. Conf. Robot. Automat.*, 2019, pp. 2838–2844.

[14] H. Zhao, J. Reher, J. Horn, V. Paredes, and A. D. Ames, "Realization of stair ascent and motion transitions on prostheses utilizing optimization-based control and intent recognition," in *Proc. IEEE Int. Conf. Rehabil. Robot.*, 2015, pp. 265–270.

[15] B. E. Lawson, H. A. Varol, A. Huff, E. Erdemir, and M. Goldfarb, "Control of stair ascent and descent with a powered transfemoral prosthesis," *IEEE Trans. Neural Syst. Rehabil. Eng.*, vol. 21, no. 3, pp. 466–473, May 2013.

[16] I. Kang, P. Kunapuli, and A. J. Young, "Real-time neural network-based gait phase estimation using a robotic hip exoskeleton," *IEEE Trans. Med. Robot. Bionics*, vol. 2, no. 1, pp. 28–37, Feb. 2020.

[17] B. Zhang et al., "An adaptive framework of real-time continuous gait phase variable estimation for lower-limb wearable robots," *Robot. Auton. Syst.*, vol. 143, 2021, Art. no. 103842.

[18] H. T. T. Vu, F. Gomez, P. Cherelle, D. Lefeber, A. Nowé, and B. Vanderborght, "ED-FNN: A new deep learning algorithm to detect percentage of the gait cycle for powered prostheses," *Sensors*, vol. 18, no. 7, 2018, Art. no. 2389.

[19] J. Lee, W. Hong, and P. Hur, "Continuous gait phase estimation using LSTM for robotic transfemoral prosthesis across walking speeds," *IEEE Trans. Neural Syst. Rehabil. Eng.*, vol. 29, pp. 1470–1477, 2021.

[20] E. J. Rouse, L. J. Hargrove, E. J. Perreault, and T. A. Kuiken, "Estimation of human ankle impedance during the stance phase of walking," *IEEE Trans. Neural Syst. Rehabil. Eng.*, vol. 22, no. 4, pp. 870–878, Jul. 2014.

[21] H. Lee, E. J. Rouse, and H. I. Krebs, "Summary of human ankle mechanical impedance during walking," *IEEE J. Transl. Eng. Health Med.*, vol. 4, pp. 1–7, 2016.

[22] W. Hong, J. Lee, and P. Hur, "Effect of torso kinematics on gait phase estimation at different walking speeds," *Front. Neurorobot.*, vol. 16, 2022, Art. no. 807826.

[23] D. Quintero, D. J. Villarreal, D. J. Lambert, S. Kapp, and R. D. Gregg, "Continuous-phase control of a powered knee–ankle prosthesis: Amputee experiments across speeds and inclines," *IEEE Trans. Robot.*, vol. 34, no. 3, pp. 686–701, Jun. 2018.

[24] S. Rezazadeh, D. Quintero, N. Divekar, and R. D. Gregg, "A phase variable approach to volitional control of powered knee-ankle prostheses," in *Proc. IEEE/RSJ Int. Conf. Intell. Robots Syst.*, 2018, pp. 2292–2298.

[25] W. Hong, N. A. Kumar, and P. Hur, "A phase-shifting based human gait phase estimation for powered transfemoral prostheses," *IEEE Robot. Automat. Lett.*, vol. 6, no. 3, pp. 5113–5120, Jul. 2021.

[26] D. J. Villarreal, D. Quintero, and R. D. Gregg, "Piecewise and unified phase variables in the control of a powered prosthetic leg," in *Proc. IEEE Int. Conf. Rehabil. Robot.*, 2017, pp. 1425–1430.

[27] T. Ma et al., "A piecewise monotonic smooth phase variable for speed-adaptation control of powered knee-ankle prostheses," *IEEE Robot. Automot. Lett.*, vol. 7, no. 3, pp. 8526–8533, Jul. 2022.

[28] X. Chen et al., "A piecewise monotonic gait phase estimation model for controlling a powered transfemoral prosthesis in various locomotion modes," *IEEE Robot. Automat. Lett.*, vol. 7, no. 4, pp. 9549–9556, Oct. 2022.

[29] M. J. Highsmith, B. W. Schulz, S. Hart-Hughes, G. A. Latlief, and S. L. Phillips, "Differences in the spatiotemporal parameters of transtibial and transfemoral amputee gait," *JPO: J. Prosthetics Orthotics*, vol. 22, no. 1, pp. 26–30, 2010.

[30] Y. Liu, K. Lu, S. Yan, M. Sun, D. K. Lester, and K. Zhang, "Gait phase varies over velocities," *Gait Posture*, vol. 39, no. 2, pp. 756–760, 2014.

[31] F. Hebenstreit, A. Leibold, S. Krinner, G. Welsch, M. Lochmann, and B. M. Eskofier, "Effect of walking speed on gait sub phase durations," *Hum. Movement Sci.*, vol. 43, pp. 118–124, 2015.

[32] W. Hong, J. Lee, and P. Hur, "Piecewise linear labeling method for speed-adaptability enhancement in human gait phase estimation," *IEEE Trans. Neural Syst. Rehabil. Eng.*, vol. 31, pp. 628–635, 2023.

[33] H.-J. Um, H.-S. Kim, W. Hong, H.-S. Kim, and P. Hur, "Design of 3D printable prosthetic foot to implement nonlinear stiffness behavior of human toe joint based on finite element analysis," *Sci. Rep.*, vol. 11, no. 1, pp. 1–11, 2021.

[34] W. Hong et al., "Empirical validation of an auxetic structured foot with the powered transfemoral prosthesis," *IEEE Robot. Automat. Lett.*, vol. 7, no. 4, pp. 11228–11235, Oct. 2022.

[35] N. A. Kumar, W. Hong, and P. Hur, "Control of a transfemoral prosthesis on sloped terrain using continuous and nonlinear impedance parameters," in *Proc. IEEE Int. Conf. Robot. Automat.*, 2021, pp. 3219–3225.

[36] K. E. Zelik and A. D. Kuo, "Human walking isn't all hard work: Evidence of soft tissue contributions to energy dissipation and return," *J. Exp. Biol.*, vol. 213, no. 24, pp. 4257–4264, 2010.

[37] K. E. Zelik, K. Z. Takahashi, and G. S. Sawicki, "Six degree-of-freedom analysis of hip, knee, ankle and foot provides updated understanding of biomechanical work during human walking," *J. Exp. Biol.*, vol. 218, no. 6, pp. 876–886, 2015.

[38] C. A. Fukuchi, R. K. Fukuchi, and M. Duarte, "A public dataset of overground and treadmill walking kinematics and kinetics in healthy individuals," *PeerJ*, vol. 6, 2018, Art. no. e4640.

[39] J. Camargo, A. Ramanathan, W. Flanagan, and A. Young, "A comprehensive, open-source dataset of lower limb biomechanics in multiple conditions of stairs, ramps, and level-ground ambulation and transitions," *J. Biomech.*, vol. 119, 2021, Art. no.110320.

[40] E. C. Honert, G. Bastas, and K. E. Zelik, "Effect of toe joint stiffness and toe shape on walking biomechanics," *Bioinspiration Biomimetics*, vol. 13, no. 6, 2018, Art. no. 066007.